Magnetic Field Effects on Chemical Reactions of Biradical Radical Ion Pairs in Homogeneous Fluid Solvents

Yukie Mori, Yoshio Sakaguchi, and Hisaharu Hayashi*

Molecular Photochemistry Laboratory, RIKEN (The Institute of Physical and Chemical Research), Wako, Saitama 351-0198, Japan

Received: February 24, 2000

Magnetic field effects (MFEs) on reactions of biradical radical ion pairs (BRIPs, $S = 3/2$ and 1/2) were investigated for the electron transfer (ET) reactions of the triplet state of 10-methylphenothiazine (^{3}MPTZ*) ($S = 1$) and electron acceptors linked with 2,2,6,6-tetramethylpiperidin-1-oxyl (TEMPO) (**A*n*−R·**) ($S = 1/2$) in various solvents by means of a nanosecond laser photolysis technique. In 2-propanol, the yield of free ions dramatically increased with increasing magnetic field (B) from 0 to 2 T, but slightly decreased from 2 to 10 T. The magnitude of the MFEs was much larger than those observed in ET reactions of ^{3}MPTZ* with acceptors without TEMPO ($S = 0$). To interpret the MFEs observed in the reactions with **A*n*−R·**, we considered the following two factors. (i) In the quenching of ^{3}MPTZ* by **A*n*−R·**, not only the ET reaction but also triplet−doublet (T−D) quenching takes place. The T−D quenching efficiency decreases with increasing B, resulting in a higher yield of BRIPs ([MPTZ$^{\bullet+}$ **A*n*$^{\bullet-}$−R·**]). However, this factor was found to have only a small contribution to the observed MFEs on the free ion yield. (ii) The ET reactions generate ^{4,2}[MPTZ$^{\bullet+}$ **A*n*$^{\bullet-}$−R·**] in quartet (Q) and doublet (D) states, which decay through either the spin-selective back ET from the D states or the separation to free ions. At $B = 0$ T, the spin conversion between the Q and D states is efficient. The increase in the free ion yield with increasing B from 0 to 2 T can be attributed to the spin relaxation from the $Q_{\pm 3/2}$ states to the $Q_{\pm 1/2}$ and $D_{\pm 1/2}$ states due to the dipole−dipole interaction of ^{3}(**A*n*$^{\bullet-}$−R·**). The slight decrease in the free ion yield with increasing B from 2 to 10 T can be attributed to acceleration of the relaxation induced by the anisotropic Zeeman interaction and/or enhancement of the $Q_{\pm 1/2}$–$D_{\pm 1/2}$ conversion induced by the difference in the isotropic g-factor between MPTZ$^{\bullet+}$ and **A*n*$^{\bullet-}$−R·**. Effects of solvents and additives on the present MFEs were also studied.

Introduction

Magnetic field effects (MFEs) on chemical reactions of radical pairs (RPs) and biradicals have been investigated extensively, and the mechanisms of these MFEs have been established by the experimental and theoretical studies.[1−3] Observation of such MFEs can give unique information about spin dynamics of paramagnetic intermediates as well as reaction mechanisms in a more general sense. Furthermore, such studies can provide the possibility to control reaction rates and/or products' selectivity by external magnetic fields. Large MFEs have been observed for RPs in micellar solutions or viscous media, where the escape of the component radicals from the solvent cage is slow enough so that the spin conversion of the RPs can take place within their lifetime. Nevertheless, a few reactions of neutral RPs in nonviscous homogeneous solutions have been reported to exhibit remarkable MFEs.[4]

Recently, magnetic interactions and spin dynamics of organic molecules of spin numbers higher than one ($S > 1$) have received increasing attention in the field of spin chemistry. By means of time-resolved EPR (TREPR) spectroscopy, novel types of spin polarization have been observed in interactions between triplet molecules and doublet radicals, these phenomena being explained in terms of the radical−triplet pair mechanism (RTPM)[5] or the electron spin polarization transfer (ESPT).[6] For a number of nitroxide-linked chromophores, EPR signals of the lowest excited quartet states have been reported, in which the triplet excited chromophore and the doublet radical are strongly coupled.[7] On the other hand, most of the studies of MFEs have dealt with chemical reactions involving doublet−doublet (D−D) pairs. MFEs on processes involving species of higher spin multiplicities in solution were scarcely reported. In fact, these studies have been limited to only photophysical processes such as triplet−triplet (T−T) annihilation and triplet−doublet (T−D) quenching.[8,9] As for theoretical studies, Johnson and Merrifield first proposed the mechanism for the MFEs of T−T annihilation in crystals.[9] Later, several researchers studied spin evolution of T−D and T−T pairs in fluid solution to interpret the MFEs on fluorescence intensity via T−T annihilation or the spin polarization due to RTPM.[10−13]

According to their theories, in the case of a pair containing at least one triplet species, its electron spin dipolar interactions play an important role in conversion between spin states with different multiplicities. Buchachenko et al. observed spin effects on the rates of radical coupling reactions through an encounter pair having three unpaired electrons and proposed that fast spin evolution should be caused by exchange interactions.[14] Owing to such interactions, it is expected that a new type of MFE can be observed for chemical reactions involving T−D or T−T pairs as intermediates. Because the spin conversions of such pairs are probably faster than those of conventional D−D pairs, MFEs on reactions of the former pairs may be observable even in fluid solutions. Thus, experimental studies on spin dynamics and magnetic field dependence of T−D or T−T pairs with chemical reaction channels have recently become a challenging area in spin chemistry.

10.1021/jp0007437 CCC: $19.00
Published on Web 04/29/2000

CHART 1

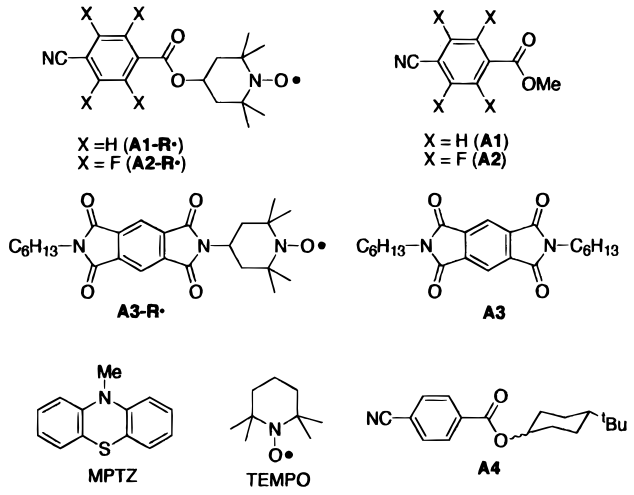

To study spin dynamics of high-spin reactive intermediates, efficient formation of such intermediates is desirable. Conti et al. reported that the excited quartet state of a nitroxide-linked fullerene undergoes an electron transfer (ET) reaction with ferrocene.[15] Our approach to the generation of intermediates having three unpaired electrons is utilization of reactions of a triplet excited molecule with a quencher covalently linked to a stable radical. Recently, we for the first time succeeded in observing MFEs on the following two chemical reactions of such T−D pairs.[16,17] (i) We found MFEs on the free ion yields in the photoinduced ET reaction of 10-methylphenothiazine (MPTZ) with an electron acceptor covalently linked to a nitroxide radical in 2-propanol (2-PrOH).[16] In this reaction, an electron was transferred from MPTZ in the lowest triplet excited state (^{3}MPTZ*) to an electron acceptor in the doublet ground state. The free ion yield increased up to 1.9-fold of that under zero field with increasing field strength (B) from 0 to 2 T. Such a large MFE is quite rare for the reactions of RPs in homogeneous fluid solutions.[4b,18] (ii) We found MFEs on the lifetime of triradicals consisting of doublet and triplet components which were generated via photochemical intramolecular H-abstraction reactions.[17] The spin relaxation rates of these triradicals were about one order larger than those of the corresponding biradicals.

In this paper, we present a full description of the work on reaction (i). To clarify the mechanism of the MFEs observed for the reactions from T−D pairs, we have investigated MFEs on the free ion yields in ET reactions of ^{3}MPTZ* with nitroxide-linked acceptors, **A*n*−R•** ($n = 1-3$, R• is TEMPO) in Chart 1. The reduction potentials of the acceptor moieties in these quenchers are varied by 0.8 eV, which can alter the rates of the forward and/or backward ET reactions. The ET reaction generates an ion-pair intermediate [$MPTZ^{\bullet+}$ $\mathbf{An}^{\bullet-}$−**R**•] in quartet (Q) and doublet (D) states. The geminate pair undergoes spin conversions between the Q and D states, backward ET, and separation to free ions. The characteristic feature of the MFEs for this three-spin system are compared with those observed in ET reactions of ^{3}MPTZ* with the corresponding spin-singlet acceptors, **A*n*** ($n = 1-3$) in Chart 1. In the quenching of ^{3}MPTZ* by **A*n*−R•**, T−D quenching also takes place in competition with ET. As a model for this T−D quenching process, MFEs on the T−D quenching by TEMPO have been examined. We propose that the MFEs observed in the reaction of ^{3}MPTZ* with **A*n*−R•** should be explained by magnetically induced changes in the spin relaxation rate of the three-spin intermediates involving each of the ET and T−D quenching processes.

Experimental Section

Chemicals. 10-Methylphenothiazine (MPTZ) and methyl 4-cyanobenzoate (**A1**) were recrystallized from ethanol. 4-(4-Cyanobenzoyloxy)-2,2,6,6-tetramethylpiperidin-1-oxyl (**A1−R•**) was synthesized as previously reported.[16] Methyl 4-cyano-2,3,5,6-tetrafluorobenzoate (**A2**) was prepared by the methods of Belf.[19] Perchlorate salt of radical cation of MPTZ ($MPTZ^{\bullet+}$ ClO_4^-) was prepared by the method of Fujita and Yamauchi.[20] The synthetic procedures for **A2−R•**, **A3−R•**, and **A4** are given in Supporting Information. Radical anions of **A1** and **A3** were prepared in MeCN by reduction of the parent compounds with Na−Hg (0.5% w/w) under vacuum in the presence of 4,7,13,-16,21,24-hexaoxa-1,10-diazabicyclo[8.8.8]hexacosane (0.025 M).[21] Anhydrous $MnCl_2$ (Aldrich, 99.99+%), $ZnCl_2$ (Kanto, analytical grade), 2,2,6,6-tetramethylpiperidin-1-oxyl (TEMPO) (Aldrich), and tetra-*n*-butylammonium tetrafluoroborate (Wako) were used as received. Acetonitrile (MeCN) (spectroscopic grade), methanol (MeOH), ethanol (EtOH), 2-propanol (2-PrOH) (Cica-Merck, HPLC grade), and 2-butanol (Kanto, analytical grade) were used as solvents for laser flash photolyses without further purification. For preparation of radical anions and electrochemical studies, dehydrated MeCN (Organics) was used as received.

Electrochemistry. Cyclic voltammetry was carried out for each sample [$(2-5) \times 10^{-4}$ M] in MeCN or 2-PrOH containing 0.1 M ^{n}Bu$_4$NBF$_4$ as the supporting electrolyte under Ar atmosphere using a BAS CV-1B voltammetry controller. Normal pulse voltammetry was carried out using a potentiostat (Hokuto Denko, HA-501) controlled by a function generator (Nippon Filcon, JJ-JOKER E−1) with a step height of 10 mV, a pulse width of 40 ms, and a pulse interval of 1 s under Ar atmosphere. Glassy carbon, Pt wire, and Ag/Ag^+ were used as working, counter, and reference electrodes, respectively.

Steady-State EPR Measurements. EPR spectra were recorded at room temperature with 100-kHz modulation on an X-band EPR spectrometer (JEOL, JES−RE1X). The magnetic fields and the microwave frequency were determined with an NMR field meter (Echo Electronics, EFM-2000AX) and a microwave counter (Echo Electronics, EMC-14), respectively. A solution of $MPTZ^{\bullet+}$ (ClO_4^-) in CH_2Cl_2 (3×10^{-4} M) was degassed by several freeze−pump−thaw cycles and sealed under vacuum. The EPR spectra of $\mathbf{A1}^{\bullet-}$ and $\mathbf{A3}^{\bullet-}$ were recorded in MeCN immediately after preparation. The spectra of TEMPO and **A*n*−R•** ($n = 1-3$) were measured in 2-PrOH (1.5×10^{-4} M) under air. The microwave power was 0.8 mW.

Laser Flash Photolyses. All of the measurements were carried out at 293 K. Each of the sample solutions was bubbled with nitrogen gas before and during experiments. The solution flowed through a quartz cell. The magnetic fields of 0−1.7 T and 0−10 T were generated by a Tokin SEE−10W electromagnet and an Oxford 37057 superconducting magnet, respectively. The third (355 nm) harmonic of a Quanta-Ray GCR-103 Nd:YAG laser was used as excitation light. As for the experiments with the TEMPO-linked acceptors, the flow rate was set high enough to avoid effects of decomposition of the acceptor due to irreversible reaction processes. For measurements of transient absorption spectra and MFEs, the concentrations of MPTZ and each of the quenchers were 1×10^{-3} M, except for the cases of **A3** and **A3−R•**. Because these imides absorb 355 nm light, a lower concentration (ca. 7×10^{-4} M) was used for them. The initial concentration of ^{3}MPTZ*

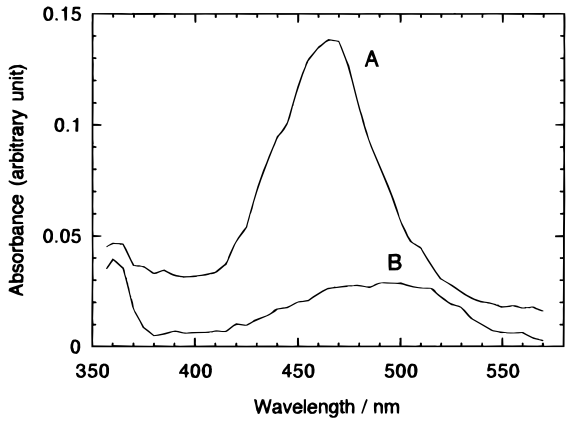

Figure 1. Transient absorption spectra of the 2-PrOH solution of MPTZ (1×10^{-3} M) and **A1**−**R**· (1×10^{-3} M) observed at (A) 35 ns and (B) 700 ns after excitation under 1 T.

generated by the laser pulse was about 1×10^{-5} M. Under these conditions, most of ^{3}MPTZ* ($\geq$ 95%) reacted with the quencher. As for global analyses of transient optical spectra, time profiles of absorbance at 40−1800 ns after excitation were recorded every 5 nm in a range of 360−750 nm. The two-dimensional data thus obtained were analyzed using the software PCPro-K.[22]

TREPR Spectrometry. TREPR measurements were carried out at room temperature on an X-band pulsed EPR spectrometer (JEOL, RSV2000) in a continuous wave mode without field modulation. The time profiles of transient signal intensities were accumulated for delay time of 0−3.5 μs after excitation at each magnetic field using a computer-controlled system.[23] The microwave power was 2−5 mW. Each of the sample solutions was deaerated by bubbling with nitrogen gas and flowed through a quartz flat or cylindrical cell with a flow rate of ca. 1.5 cm^3 min^{-1}. The sample was excited with the third harmonic (355 nm) of a Quanta-Ray GCR-3 Nd:YAG laser with a repetition rate of 30 Hz.

Results and Discussion

Reaction Scheme. To clarify reaction pathways to give the free ions in the quenching of ^{3}MPTZ* by **An**−**R**·, the dynamic behaviors of the intermediates were examined by means of transient absorption spectroscopy and TREPR. For comparison, similar experiments were also carried out with **An** and TEMPO.

Transient Absorption Spectroscopy. When a 2-PrOH solution of MPTZ and **A1**−**R**· was irradiated with a 355-nm laser pulse, the transient absorption spectrum recorded immediately after excitation showed an absorption band around 465 nm, which was ascribed to the T−T absorption of MPTZ[24] (Figure 1, trace A). After this band decayed, the transient spectrum showed a broad band around 500 nm and a sharp peak at 360 nm (Figure 1, trace B). This spectrum can be regarded as the superposition of the absorption spectra due to MPTZ$^{\bullet+}$ (λ_{max} 515 and 445 nm (shoulder)[24,25]) and **A1**$^{\bullet-}$−**R**· (λ_{max} 480 and 357 nm for **A1**$^{\bullet-}$ in MeCN). When **A2**−**R**· or **A3**−**R**· was used as the electron acceptor, the spectrum due to MPTZ$^{\bullet+}$ and the biradical anion (λ_{max} = 455 and 353 nm for **A2**$^{\bullet-}$−**R**·; 725 and 650 nm for **A3**$^{\bullet-}$−**R**·) was also observed after the decay of ^{3}MPTZ*. These results indicate that the ET reaction between ^{3}MPTZ* and **An**−**R**· (n =1−3) gave a biradical radical ion pair (^{4,2}BRIP)

$$^3\text{MPTZ}^* + \mathbf{An}-{}^2\mathbf{R}\cdot \rightarrow {}^{4,2}[\text{MPTZ}^{\bullet+}\ \mathbf{An}^{\bullet-}-\mathbf{R}\cdot]\ (^{4,2}\text{BRIP}) \quad (1)$$

When **An** (n =1−3) was used as the acceptor, the observed spectral changes were similar to those observed in the reactions with **An**−**R**·. The intensities of the absorption bands due to the radical ions were larger than those observed in the reactions with **An**−**R**·. The primary ET product with **An** is a triplet radical ion pair (^{3}RIP)

$$^3\text{MPTZ}^* + \mathbf{An} \rightarrow {}^3[\text{MPTZ}^{\bullet+}\ \mathbf{An}^{\bullet-}]\ (^3\text{RIP}) \quad (2)$$

Similar ET reactions of ^{3}MPTZ* with 1,4-dicyanobenzene (DCNB) and 2,3,5,6-tetrafluoro-1,4-dicyanobenzene (F_4DCNB) were also reported.[26]

In the quenching of ^{3}MPTZ* by TEMPO, no transient absorption band assignable to any other intermediates was observed after the decay of the T−T absorption. The absence of the absorption due to MPTZ$^{\bullet+}$ suggests that ^{3}MPTZ* was quenched by TEMPO through not ET but another process. It is known that an excited triplet molecule can be quenched by a doublet radical through an energy transfer, when this process is exothermic.[8c,27] The lowest excitation energy of TEMPO in 2-PrOH was estimated to be about 2.3 eV,[28] which is lower than the triplet energy (2.64 eV[24]) of MPTZ. It is likely that the excitation energy would be transferred from ^{3}MPTZ* to TEMPO in the T−D quenching process

$$^3\text{MPTZ}^* + {}^2\text{TEMPO} \rightarrow \text{MPTZ}\ (S_0) + {}^2\text{TEMPO}\ (D_1 \text{ and/or } D_0) \quad (3)$$

TREPR Spectroscopy. Figure 2A shows the TREPR spectrum observed in the reaction of ^{3}MPTZ* with **A1**−**R**· in 2-PrOH. In this figure, three sharp emissive signals with a line separation of 1.6 mT and a broad absorption one were observed.[29] The former ones were assigned to the TEMPO part in **A1**−**R**· (a_N = 1.59 mT). The broad signal may be due to MPTZ$^{\bullet+}$ generated by ET to the acceptor. The center of the broad signal was observed at a field higher than that of the emissive signals, which is consistent with fact that the g-factor of MPTZ$^{\bullet+}$ (2.0052) is smaller than that of TEMPO part in **A1**−**R**· (2.0062). The TREPR spectrum of a 2-PrOH solution containing MPTZ (2×10^{-3} M) and **A3**−**R**· (7×10^{-4} M) also showed net emissive signals due to the TEMPO moiety.[29]

Figure 2B shows the TREPR spectrum on excitation of MPTZ in the presence of TEMPO (1×10^{-3} M) in 2-PrOH. An emissive three-line signal with an intensity ratio of almost 1:1:1 and a line separation of 1.6 mT was observed, which was assigned to the signal due to TEMPO (a_N = 1.60 mT). The emissive signal disappeared within 1.5 μs, which corresponded to the spin−lattice relaxation to the thermal equilibrium.[30] The observed net emissive polarization of the signals due to TEMPO or the TEMPO moiety in **An**−**R**· is explained in terms of the quartet precursor RTPM with a negative J value.[5] The results of transient absorption spectroscopy and the TREPR measurements showed that ^{3}MPTZ* was quenched by **An**−**R**· in 2-PrOH through both ET to the acceptor moiety (**An**) (process 1) and the T−D interaction by the radical (**R**·) (process 4)

$$^3\text{MPTZ}^* + \mathbf{An}-{}^2\mathbf{R}\cdot \rightarrow \text{MPTZ}\ (S_0) + \mathbf{An}-\mathbf{R}\cdot\ (D_0 \text{ and/or } D_1) \quad (4)$$

Quenching Rate Constants. The quenching rate constants (k_q's) of ^{3}MPTZ* by the above quenchers in 2-PrOH at 293 K are listed in Table 1. For all quenchers except TEMPO, the k_q values were close to the diffusion-control limit in 2-PrOH. The k_q value increased in the following order among the acceptors of a similar size: **A1** < DCNB < **A2** < F_4DCNB. The free

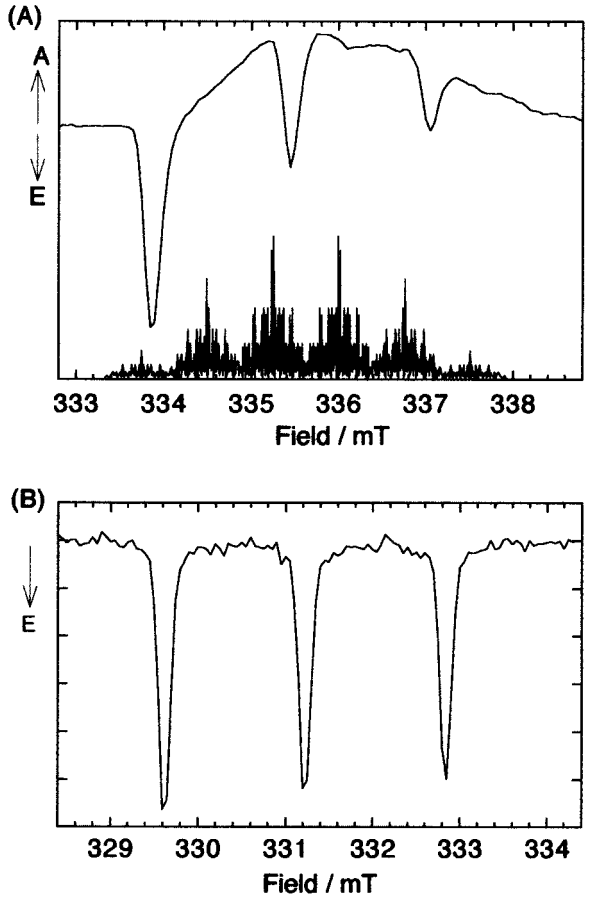

Figure 2. TREPR spectra observed on excitation of the 2-PrOH solutions of MPTZ (1×10^{-3} M) in the presence of (A) **A1**−**R**· (1×10^{-3} M) and (B) TEMPO (1×10^{-3} M) at 355 nm. The detection periods are (A) 200−400 ns and (B) 300−600 ns, respectively, after the laser pulse. The lower trace in (A) is the stick diagram of the EPR spectrum of $MPTZ^{\bullet+}$ ($g = 2.0052$, $a_N = 0.765$ mT, $a_H = 0.742$ mT × 3, 0.213 mT × 2, 0.113 mT × 2, 0.070 mT × 2, 0.023 mT × 2).[26]

energy changes accompanying this ET process (ΔG_{ET}) were estimated to be −0.35, −0.40, −0.82, and −1.01 eV for **A1**, DCNB, **A2**, and F_4DCNB, respectively, with the Rehm−Weller equation.[31] This means that the more exothermic the reaction is, the faster it proceeds. Despite a more negative ΔG_{ET} value (−1.16 eV) for the reaction of **A3** than those of F_4DCNB and **A2**, its k_q value was somewhat lower than those of the latter reactions. This is probably explained by the smaller diffusion coefficient due to the larger molecular size of **A3** than those of F_4DCNB and **A2**, indicating that the k_q value reached the diffusion-control limit in such a highly exothermic case as the reaction of **A3**. This energy gap dependence of k_q agreed with the Rehm−Weller relationship.[31b]

The k_q values for **A*n***−**R**· ($n = 1-3$) were similar to those for **A*n***, as shown in Table 1. It should be noted that the k_q values for **A*n***−**R**· include contributions from both the ET reaction (process 1) and the T−D quenching (process 4). They cannot be separated into the rates of the respective processes. Because the rate of the T−D quenching by TEMPO was less than half of the ET reaction rates with **A*n***, the ET process probably dominated the T−D quenching in the quenching by **A*n***−**R**·.

MFEs on Free Ion Yields. *Dynamic Behaviors of Ion Pair Intermediates*. Figure 3A shows the time profiles of the transient absorbance at 520 nm ($A_{520}(t)$ curves) observed for the reaction of ^{3}MPTZ* with **A1** in 2-PrOH at 293 K in the absence and presence of magnetic fields. Because ^{3}MPTZ* was almost completely quenched within 1 μs, each of the $A_{520}(t)$ curves at $t > 1$ μs was mainly ascribed to the absorption of $MPTZ^{\bullet+}$ with a smaller contribution from the absorbance due to $\mathbf{A1}^{\bullet-}$. As is shown in Scheme 1, the geminate ^{3}RIP decays unimolecularly either by the intrapair backward ET through a singlet channel (process f) after the T−S conversion (process e) or by the separation to free ions (process g).

Here, the efficiency of free ion formation (ϕ_{FI}) through an ion pair (IP) in the quenching of ^{3}MPTZ* by a quencher (Q) is defined as follows:

$$\phi_{FI} \equiv (\text{number of free } MPTZ^{\bullet+} \text{ formed})/(\text{total number of } ^3\text{MPTZ* quenched by Q}) = \phi_{IP} \times \phi_{sep} \quad (5a)$$

$$\phi_{IP} = (\text{number of geminate IP formed})/(\text{total number of } ^3\text{MPTZ* quenched by Q}) \quad (5b)$$

$$\phi_{sep} = (\text{number of free ions formed})/(\text{number of geminate IP formed}) \quad (5c)$$

The ϕ_{FI} values in the reactions with **A1**, **A3**, DCNB, and F_4-DCNB under zero field were estimated with the reported ϵ values[32] for ^{3}MPTZ* and $MPTZ^{\bullet+}$ and listed in Table 1.[33] The

TABLE 1: Redox Potentials (E) of the Reactants, Quenching Rates (k_q) of the Reactions of ^{3}MPTZ* with Various Quenchers, and Efficiencies for Free Ion Formation (ϕ_{FI}) of the Reactions

	E/V[a](in MeCN)		$k_q/10^9$ M^{-1} s^{-1} [d]	ϕ_{FI}[e]
compd	reversible[b]	irreversible[c]	(in 2-PrOH)	(in 2-PrOH)
MPTZ	0.315 (0.32)[f]			
A1	−2.06 (−2.055)[f]		3.9	0.56[g] (0.62[h])
A1−**R**·	−2.075	−1.755[i]	4.1	0.18
A2	−1.60		5.5[j]	*k*
A2−**R**·	−1.583	−1.76	4.8[j]	*k*
A3	−1.26		5.3[j]	0.38
A3−**R**·	−1.233	−1.78	5.0[j]	0.20
TEMPO		−1.91(−1.75)[f]	1.9	∼0
DCNB	−2.018 (−2.023)[e]		4.6 [l]	0.71
F_4DCNB	−1.41		5.9 [l]	0.66

[a] Versus ferrocene. The scan rate was 50 mV s^{-1}. [b] $E_{1/2}$. The peak separations were 60−70 and ca. 100 mV in MeCN and 2-PrOH, respectively. [c] Peak potential in cathodic scan. [d] The k_q values were obtained at 293 K under 0 T from the slope of the straight line in the Stern−Volmer plots in a concentration range of $(0.6-1.5) \times 10^{-3}$ M. [e] The ϕ_{FI} values were obtained at 293 K under 0 T. [f] The values in parentheses were measured in 2-PrOH. [g] Based on ϕ_{FI} (**A1**)/ ϕ_{FI} (**A1**−**R**·) = 3.1. [h] Based on ϕ_{FI} (**A1** in 2-PrOH)/ ϕ_{FI} (**A1** in MeCN) = 0.67. In MeCN, ϕ_{FI} (**A1**) was assumed equal to ϕ_{FI} (DCNB). [i] The $E_{1/2}$ value was determined to be −1.83 V in MeCN by normal pulse voltammetry. [j] The k_q values were measured at only one concentration. [k] Not determined, but ϕ_{FI} (**A2**)/ ϕ_{FI} (**A2**−**R**·) ∼ 3. [l] Reference 26.

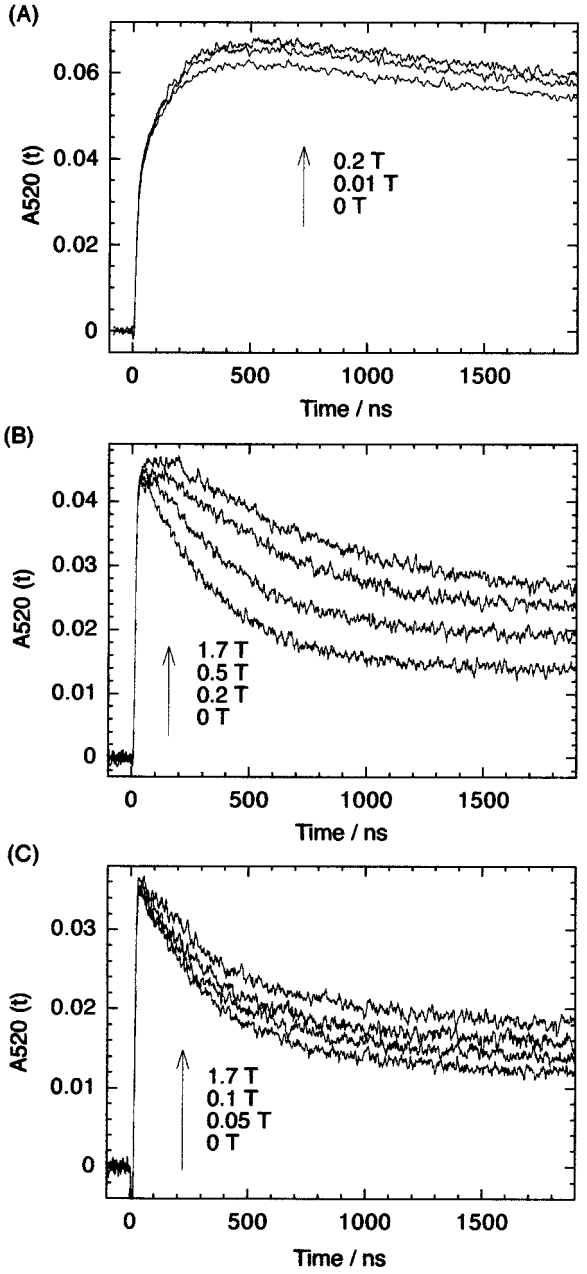

Figure 3. $A_{520}(t)$ curves observed in the reactions of ^{3}MPTZ* with (A) **A1** (1×10^{-3} M), (B) **A1**−**R**· (1×10^{-3} M), and (C) **A3**−**R**· (7×10^{-4} M) in 2-PrOH. The *B* values are shown in the figure.

ϕ_{sep} value for the reaction of ^{3}MPTZ* with **A***n* is determined by the relative magnitude of the rates of processes e−g in Scheme 1. According to the method of Sano and Tachiya,[34] the rate of separation to free ions (k_{sep}) for IP consisting of oppositely charged univalent ions is estimated from eq 6[35]

$$k_{sep} = D_r r_c r_q^{-3} [\exp(r_c/r_q) - 1]^{-1} \quad (6a)$$

$$r_c = e^2/4\pi\epsilon_0\epsilon_r kT \quad (6b)$$

where D_r, r_c, and r_q are the mutual diffusion coefficient, the Onsager distance, and the quenching distance, respectively. The k_{sep} value for [MPTZ$^{\bullet+}$ **A***n*$^{\bullet-}$] in 2-PrOH at 293 K is calculated to be 9×10^7 s^{-1}, when the r_q value was assumed to be 8 Å. D_r was estimated to be 5.6×10^{-10} m^2 s^{-1} by the Stokes−Einstein relation with ionic radii of 3.5 and 3.0 Å for MPTZ$^{\bullet+}$ and **A***n*, respectively.[36] Because the estimated k_{sep} value is much

SCHEME 1. Pathways of Formation and Decay of RIP in the Reaction of ^{3}MPTZ* with A*n* where k_d Is the Diffusion-Controlled Rate and Arrows: a, Separation to Each Component; d, Forward ET; e, T−S Conversion of RIP; f, Backward ET; g, Separation to Free Ions; h, Random Encounter of the Free Ions

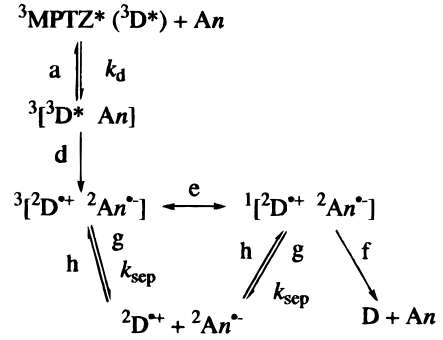

SCHEME 2. Pathways of Formation and Decay of BRIP in the Reaction of ^{3}MPTZ* with A*n*−R· and Arrows: b, Quenching to the S_0 State; c, Q−D Conversion of the Encounter Complex; e′, Q−D Conversion of BRIP and Other Symbols Have the Same Meanings as in Scheme 1

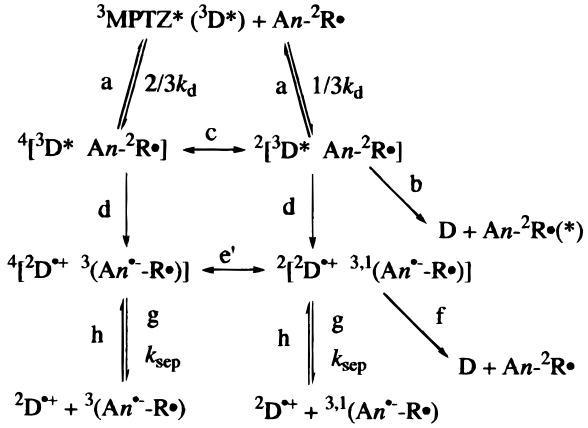

larger than the observed decay rate ($(4-6) \times 10^6$ s^{-1}) of ^{3}MPTZ* in the bimolecular quenching under the conditions employed, separation of the kinetics of the geminate decay of RIP from that of its formation seems impossible. Indeed, each of the $A_{520}(t)$ curves in Figure 3A decayed with second-order kinetics at $t > 1$ μs, which corresponds to the random bimolecular recombination of the free ions (processes h, e, and f in Scheme 1).[37]

Next, the reactions of ^{3}MPTZ* with **A***n*−**R**· were examined under the same conditions. The reaction pathways of BRIP are considered as analogous to those of RIP, as is shown in Scheme 2 (processes e′−g). Figures 3B and 3C show the $A_{520}(t)$ curves observed in the reactions of ^{3}MPTZ* with **A***n*−**R**· (n =1 or 3) in the absence and presence of magnetic fields. Because the absorbance due to **A3**$^{\bullet-}$−**R**· at 520 nm was negligibly small, the $A_{520}(t)$ curves in Figure 3C were almost exclusively due to MPTZ$^{\bullet+}$, except in their initial stage. In the reactions with **A***n*−**R**·, the ϕ_{FI} values under zero field were much smaller than that observed in the reaction with **A***n* (Table 1).[38] As shown in Figure 3, however, the magnetically induced changes in ϕ_{FI} were much larger in the reactions with **A***n*−**R**· than those observed in the reactions with **A***n*.

MFEs on the ϕ_{FI} Value. As a measure of the MFEs on ϕ_{FI}, the *R(B)* value defined as $R(B) = A_{520}(t, B)/A_{520}(t, 0\ \text{T})$ will be used hereafter ($t = 1.8$ μs for the reaction with **A1**−**R**· and $t =$

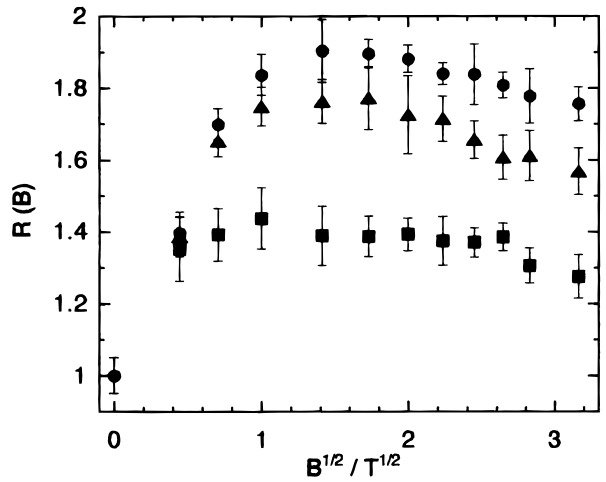

Figure 4. $R(B)$ vs $B^{1/2}$ plots in the reactions of ^{3}MPTZ* with **A1**−**R**· (●), **A2**−**R**· (▲), and **A3**−**R**· (■) in 2-PrOH. The error bars indicate $\pm\sigma$. For **A1**−**R**·, $R(B) = A_{520}(1.8\ \mu s, B)/A_{520}(1.8\ \mu s, 0\ T)$; for others, $R(B) = A_{520}(1\ \mu s, B)/A_{520}(1\ \mu s, 0\ T)$.

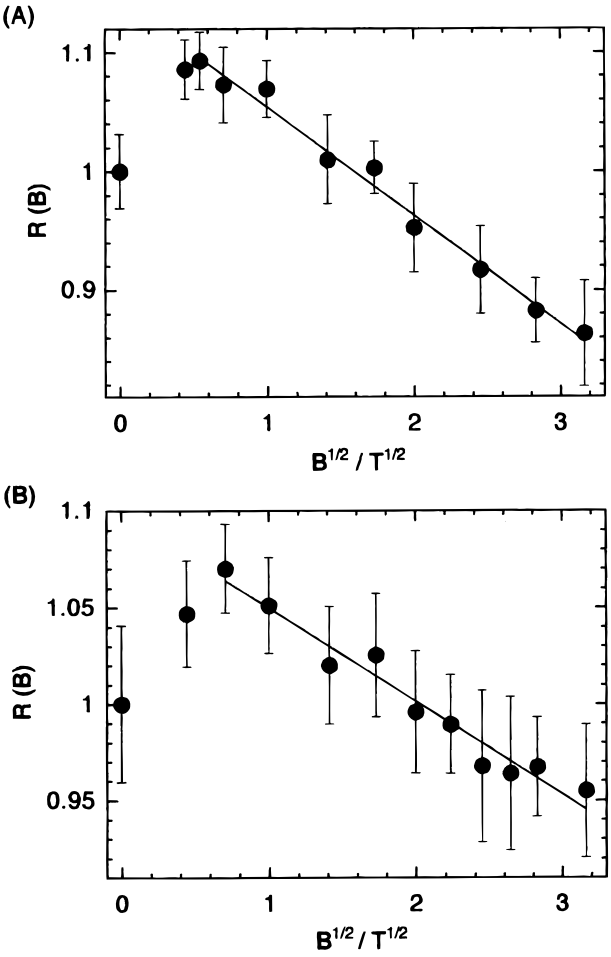

Figure 5. $R(B)$ vs $B^{1/2}$ plots in the reactions of ^{3}MPTZ* with (A) **A1** and (B) **A3** in 2-PrOH. The solid lines are the least-squares fitted lines with the data at $B = 0.5-10$ T. The error bars indicate $\pm\sigma$.

1 μs for those with **An**, **A2**−**R**·, and **A3**−**R**·). Because the ET and the successive geminate processes were completed within 1 μs, the *R(B)* value can be regarded as the ratio of $\phi_{FI}(B)/\phi_{FI}(0\ T)$.[39] Figures 4 and 5 show the plots of *R(B)* against $B^{1/2}$ for the reactions of ^{3}MPTZ* with **An**−**R**· and **An**, respectively. The plots for **A2** (not shown) were quite similar to those for **A1**. Characteristic features of the MFEs on the *R(B)* values observed in these reactions are summarized as follows: (i) The magnitude of MFEs on *R(B)* for **An**−**R**· was much larger than that for **An**, and the field dependences were also different from each other. (ii) As is seen in Figure 4, the *R(B)* values for **An**−**R**· dramatically increased with increasing B from 0 T to 1−2 T, but slightly decreased from 2 to 10 T. (iii) The maximal *R(B)* value increased in the order of **A3**−**R**· < **A2**−**R**· < **A1**−**R**·. The R(2 T) value of 1.9 for **A1**−**R**· was quite large in MFEs observed for reactions in homogeneous fluid solutions at room temperature. (iv) As is seen in Figure 5, the *R(B)* values for the reactions with **An** increased by 7−10% with increasing B from 0 T to 0.2−0.5 T. At higher fields than 0.5 T, they decreased with increasing B and became 0.88−0.95 at 10 T. In a range of $0.5 < B < 10$ T, the *R(B)* vs $B^{1/2}$ plots gave a straight line in each case.

These MFEs on *R(B)* observed for the reactions of **An** can be explained by combination of the hyperfine coupling mechanism (HFCM) and the Δg mechanism (ΔgM), as was previously reported for the reactions of ^{3}MPTZ* with DCNB or F_4DCNB.[26] The smaller slope of the straight line for **A3** than that for **A1** is ascribed to the smaller Δg value ($g(\text{MPTZ}^{\bullet+}) - g(\mathbf{A3}^{\bullet-}) = 0.0011$) of the former RIP than that ($g(\text{MPTZ}^{\bullet+}) - g(\mathbf{A1}^{\bullet-}) = 0.0020$) of the latter one. Now, it is clear that the MFEs on ϕ_{FI} observed for the reactions of **An**−**R**· should be interpreted by a different mechanism from those for **An**. From eq 5a, *R(B)* is represented by

$$R(B) = [\phi_{FI}(B)/\phi_{FI}(0\ T)] = [\phi_{IP}(B)/\phi_{IP}(0\ T)] \times [\phi_{sep}(B)/\phi_{sep}(0\ T)] \quad (7)$$

There are two possible explanations for the difference in observed MFEs between the reactions of **An**−**R**· and those of **An**. (i) In the former case, ϕ_{IP} may be largely dependent on B, because the T−D quenching takes place in competition with the formation of BRIP, while in the latter one ϕ_{IP} is independent of B. (ii) MFEs on ϕ_{sep} for BRIP may be quite different from those for RIP.

MFEs on T−D Quenching. To get information on the B-dependence of ϕ_{IP}, we examined MFEs on the T−D quenching rate of ^{3}MPTZ* by TEMPO as a model of the T−D quenching by **An**−**R**·. The k_q value[40] of the T−D quenching by TEMPO in 2-PrOH decreased from 1.9×10^9 M^{-1} s^{-1} to 1.6×10^9 M^{-1} s^{-1} with increasing B from 0 to 6 T and became constant at $B = 6-10$ T (Figure S1). The asymptotic variation of k_q is similar to the field dependence of the T−D quenching in the electrochemiluminescence (ECL) reactions reported by Bard et al.[8a,b] They reported that the ECL of aromatic compounds such as rubrene was enhanced by 5−30% at $B = 0.8$ T in comparison with that at $B = 0$ T. The ECL intensities were monotonically increased from 0 to 0.8 T. At $B = 0.8$ T, they were either almost saturated or still increasing. The increase in ECL intensity indicates that magnetic fields suppressed the T−D quenching of the excited triplet state of the aromatic compounds by the radical ions existing in the electrolytic solutions.

These MFEs can qualitatively be explained in terms of the quenching scheme by Johnson and Merrifield[9] (Scheme 3), where ^{3}M* and ^{2}R· stand for an excited triplet state molecule and a doublet species, respectively. On a collision of ^{3}M* and ^{2}R·, the overall spin of the pair is in the Q or D state with a statistical ratio of 2:1. Spin-selective quenching through a doublet channel (process b) causes depletion of the pair in the D state. If the Q and the D states are nearly degenerate, the electron spin dipolar interaction of ^{3}M* induces the Q−D conversion (process c), which regenerates population in the D

SCHEME 3. T−D Quenching Scheme of a Triplet Molecule (^{3}M*) with a Radical (^{2}R·) (symbols have the same meanings as in Schemes 1 and 2)

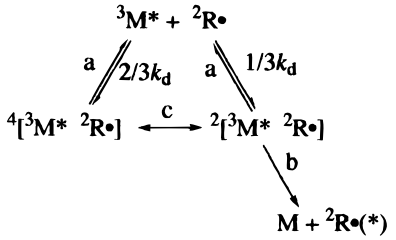

state. Under a magnetic field much larger than the zero-field splitting ($|D|$) of ^{3}M*, the $Q_{\pm 3/2}$ states are energetically isolated from the $Q_{\pm 1/2}$ and $D_{\pm 1/2}$ states by the Zeeman interaction. Thus, the Q−D conversion from the $Q_{\pm 3/2}$ states is prohibited by large magnetic fields. Parallel to processes b and c, the pair can separate to unquenched ^{3}M* and ^{2}R· (process a). If the Q−D conversion is diminished by magnetic fields, the apparent quenching rate (k_q) of ^{3}M* is also decreased.

To get a more realistic model for the T−D quenching in fluid solutions, Atkins and Evans modified the above theory by taking rotational and translational motions into account.[11] In their theory, they assumed that the collision is short-lived and that the Q−D conversion of the T−D pair is ceased during the collision by a large exchange interaction. Instead, the spin relaxation of ^{3}M* and ^{2}R· composing a T−D pair in the Q state is considered to occur independently while they are at a distance such that the exchange interaction is negligibly small. Some of them may escape from the so-called "solvent cage", which means the decomposition of the T−D pair. However, if ^{3}M* and ^{2}R· approach each other again, they collide in the D state with a certain probability. Usually, the spin relaxation of ^{3}M* is more important in the Q−D conversion than that of ^{2}R·, because the former is much faster than the latter. The rate of the spin relaxation of ^{3}M* induced by the electron spin dipolar interaction was shown to decrease with increasing B, based on the Redfield theory.[41] Using such a model, they demonstrated that the T−D quenching efficiency decreased with increasing B and that the efficiency approached an asymptotic value of the high-field limit. The MFEs on k_q observed for the quenching of ^{3}MPTZ* by TEMPO can be explained in terms of this theory.

Next, MFEs on the k_q values observed in the reactions of ^{3}MPTZ* with **An**−**R**· were examined. In the reaction with **A2**−**R**·, the k_q value decreased only by 3% with increasing B from 0 to 2 T and became constant within the experimental error (<1%) at B = 2−10 T. As for **A1**−**R**·, the k_q value also decreased by 3% with increasing B from 0 to 1.7 T. These MFEs were smaller than that observed for TEMPO (16% decrease in k_q). The smaller magnitude of MFEs in the quenching by **An**−**R**· than that in the quenching by TEMPO can be explained from comparison of the decay pathways of [^{3}MPTZ* **An**−**R**·] (Scheme 2) with the T−D quenching scheme (Scheme 3). In addition to processes a−c, the competitive ET (process d of Scheme 2) gives another decay route of the encounter pair which is not included in Scheme 3. Considering that the ET reaction with **An** is faster than the T−D quenching by TEMPO (Table 1), we can assume that most part of [^{3}MPTZ* **An**−**R**·] borne in the Q state should decay through ET rather than through the conversion to the D state. In such a case, if the conversion from ^{4}[^{3}MPTZ* **An**−**R**·] to ^{2}[^{3}MPTZ* **An**−**R**·] is suppressed by magnetic fields, the yield of the S_0 state of MPTZ only slightly decreases, whereas that of BRIP slightly increases. Thus, it is reasonable that the magnitude of MFEs on the k_q value in the reactions of ^{3}MPTZ* with **An**−**R**· is smaller than that in the T−D quenching without any competitive process.

Mechanism of MFEs on *R(B)* in the Reaction of ^{3}MPTZ* with An-R·. The above discussion indicates that the magnetically induced increases in the *R(B)* values observed for the reactions of ^{3}MPTZ* with **An**−**R**· (Figure 4) are partially attributed to the suppression of the T−D quenching but that this contribution to the present MFEs is quite small. Let us consider the second possibility, that is, the B-dependence of ϕ_{sep} for BRIP.

Q−D Conversion of BRIP. The field dependence of *R(B)* in the reactions of ^{3}MPTZ* with **An**−**R**· (Figure 4) is similar to that of the lifetime reported for RPs in micellar solutions[2,10d,42] or biradicals linked by flexible chains.[3,43] In such confined media, the lifetime of RPs is long enough for spin relaxation to take place. In these reports, the authors explained the observed MFEs by the relaxation mechanism[44] (RM). According to the theory of RM, under high magnetic fields ($B \gg |A_{HFC}|, |J|$), where the $T_{\pm 1}$ states are separated from the S and T_0 states, the $T_{\pm 1}$−S and $T_{\pm 1}$−T_0 conversions occur through the spin relaxation. Spin relaxation of RPs is induced by intra-radical anisotropic HFC and Zeeman interactions and inter-radical electron spin dipolar interactions[1−3,42,43] which are modulated by rotational motion of the radicals and/or fast intramolecular local motion such as torsional vibration.[43a] If only the S state gives products, the lifetime of RP in the $T_{\pm 1}$ states is substantially determined by the spin relaxation rate (k_{rlx}). In homogeneous fluid solutions, however, MFEs due to the RM are hardly observed for RPs consisting of typical organic radicals, because k_{sep} is much larger than k_{rlx} (10^5−10^6 s^{-1}). Indeed, the MFEs on *R(B)* observed in the reactions of ^{3}MPTZ* with **An** were attributed to the HFCM and ΔgM rather than the RM, as was discussed above.

If the MFEs observed in the reactions of ^{3}MPTZ* with **An**−**R**· are due to the RM, the k_{rlx} values of ^{4,2}BRIPs should be much larger than those of ^{3,1}RIPs. In our previous work, the MFEs on the decay rates of the triradicals were explained by the RM.[17] The k_{rlx} values (10^6−10^7 s^{-1}) of the triradicals were about one order higher than those of the corresponding biradicals at $0 < B \leq 10$ T. The larger k_{rlx} values of the triradicals are probably attributed to the electron spin dipolar interactions between the two radical centers within the triplet components. As was discussed above, the MFEs on the k_q value in the T−D quenching of ^{3}MPTZ* by TEMPO can also be attributed to the B-dependence of the spin relaxation rate induced by the electron spin dipolar interaction of ^{3}MPTZ*. For the present BRIPs, the observed MFEs on $R(B)$ can also be explained by the RM.[45] At low fields ($B \leq |D'|, |J|$), the Q−D conversion of BRIPs (process e′) is fast enough so that a part of the BRIPs borne in the Q_m ($m = \pm 1/2, \pm 3/2$) states is converted to the $D_{m'}$ ($m' = \pm 1/2$) ones before the separation to free ions (process g). Here, D' is one of the zero-field parameters of **An**$^{\bullet-}$−**R**·. As B increases, the $Q_{\pm 3/2}$ states are energetically isolated from the $Q_{\pm 1/2}$ and $D_{\pm 1/2}$ states by the Zeeman interaction, and the spin relaxation induced by the electron spin dipolar interaction within **An**$^{\bullet-}$−**R**· becomes slower. As a result, the conversion from the $Q_{\pm 3/2}$ states to the $Q_{\pm 1/2}$ or $D_{\pm 1/2}$ ones is reduced, leading to an increase in ϕ_{sep}. On the other hand, the relaxation induced by the anisotropy of the g-tensor is accelerated with increasing B, approaching an asymptotic value at ultrahigh fields. The slight decrease of $R(B)$ with B at 2−10 T may be attributed to the increase in k_{rlx} due to this mechanism. More remarkable reversion of MFE was reported for RPs in micellar solutions[42b,c] and chain-liked biradicals.[43a] In those cases, it was suggested

TABLE 2: Solvent Effects on $R(B)$ in the Reaction of ^{3}MPTZ* with A1−R· at 293 K

solvent	ϵ_r[a]	η / cP[a]	R(1.7 T)
MeCN	36.64	0.369[b]	1.0
MeOH	33.0	0.611	1.08
MeOH−ethylene glycol (1:1)			1.23
EtOH	25.3	1.19	1.28
2-PrOH (containing 0.05 M ^{n}Bu$_4$NBF$_4$)			1.62
2-PrOH	20.18	2.39	1.85
2-butanol	17.93	3.096[b]	2.57

[a] Reference 54. [b] At 298 K.

that the relaxation induced by the *g*-tensor anisotropy is important and that the correlation time for its modulation is relatively short. In the present case, the spin relaxation is induced mainly by the electron spin dipolar interactions. Thus, it is not surprising that the MFEs on $R(B)$ exhibited only small reversion. Alternatively, the decrease in $R(B)$ with increasing B from 2 to 10 T may be attributed to the acceleration of the $Q_{\pm1/2} - D_{\pm1/2}$ due to the difference in the isotropic *g*-factor between the triplet and the doublet components, as was proposed by Atkins and Evans.[11]

Let us compare the spin dynamics between the two types of T−D pair, [^{3}MPTZ* ^{2}R·] and [^{2}MPTZ$^{\bullet+}$ ^{3}(**An**$^{\bullet-}$−**R**·)]. The similarities and differences are summarized as follows. (i) In both the cases, the consumption of the reactants occurs through the pair in the D state,[46] and the pair in the Q state is inactive. (ii) The RM can account for both the MFEs on k_q for [^{3}MPTZ* ^{2}R·] and those on $R(B)$ for [^{2}MPTZ$^{\bullet+}$ ^{3}(**An**$^{\bullet-}$−**R**·)]. Under high magnetic fields ($B \gg |J|$, $|D|$, or $|D'|$), the $Q_{\pm3/2}$ states are converted to the $Q_{\pm1/2}$ or $D_{\pm1/2}$ states through the spin relaxation, which is mainly induced by the electron spin dipolar interactions of the triplet components. (iii) It was reported that the D^* ($= (D^2 + 3E^2)^{1/2}$) value for the lowest excited triplet state of unsubstituted phenothiazine is 0.1296 cm^{-1} ($D^*/g\beta$ = ca. 138 mT) in polyethylene matrix at 77 K.[47] The $|D'|$ value of **A3**$^{\bullet-}$−**R**· was estimated to be 4.35 mT using the point−dipole approximation with the distance between the midpoint of the N−O bond and the center of the benzene ring (d_{CC}).[48] As for **A1**$^{\bullet-}$−**R**·, the $|D'|$ values of 4.64 and 9.28 mT were obtained for the extended (with the torsion angle of the ester linkage ϕ[C−C(=O)−O−C] = ca. 180°; d_{CC} = 8.44 Å) and the folded (ϕ = ca. 0°; d_{CC} = 6.99 Å) conformers, respectively. These facts suggest that the $|D'|$ values of **An**$^{\bullet-}$−**R**· are much smaller than the $|D|$ value of ^{3}MPTZ*. (iv) The time scale of the fluctuation of the electron spin dipolar interaction is determined by the correlation times (τ_C). If the rotation of the triplet species as a whole molecule is responsible for the fluctuation, the τ_C values of ^{3}MPTZ* and **An**$^{\bullet-}$−**R**· are probably similar to each other. For **A1**$^{\bullet-}$−**R**· and **A2**$^{\bullet-}$−**R**·, the rotation about the C−O bond in the ester linkage causes large variation of the inter-radical distance. Such an intramolecular motion can also contribute the fluctuation of this interaction. (v) The magnitude of the MFEs on $R(B)$ for [MPTZ$^{\bullet+}$ ^{3}(**An**$^{\bullet-}$−**R**·)] is much larger than that on k_q for [^{3}MPTZ* ^{2}R·]. This difference may be attributed to the longer lifetime of the former pair.[49] The larger $|D|$ of [^{3}MPTZ* ^{2}R·] causes the more efficient Q−D conversion, but the lifetime of pairs is also an important factor determining the magnitude of MFEs.

Effects of Solvents and Additives. According to eq 6, alteration of solvent properties can vary k_{sep}, which in turn affects ϕ_{sep}. Furthermore, addition of a neutral salt such as tetra-*n*-butylammonium tetrafluoroborate (^{n}Bu$_4$NBF$_4$) sometimes accelerates the separation of IP.[50] For the reaction of ^{3}MPTZ* with **A1**−**R**·, MFEs on $R(B)$ were examined in various solvents (Table 2) at

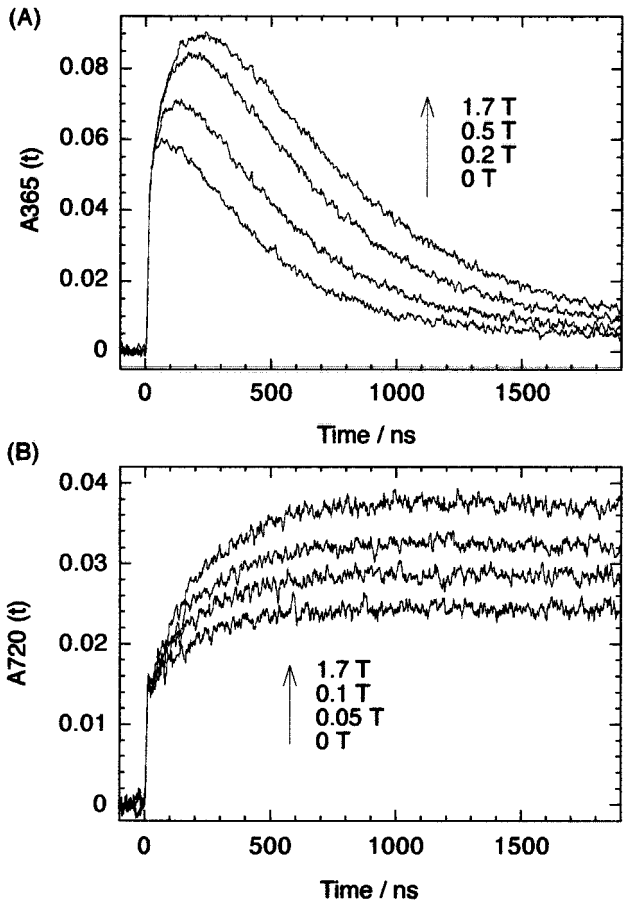

Figure 6. (A) $A_{365}(t)$ curves observed for the same reaction as Figure 3B. (B) $A_{720}(t)$ curves observed for the same reaction as Figure 3C. The B values are shown in the figure.

fields below 1.7 T. In each of the solvents except MeCN, $R(B)$ monotonically increased with B from 0 to 1.7 T. In MeOH and EtOH, the MFEs were saturated at ca. 1 T. A comparison of the intensities of the transient absorption due to MPTZ$^{\bullet+}$ showed that ϕ_{FI} decreased from the top to the bottom for the solvents listed in Table 2. These results indicate that ϕ_{FI} increases and $R(B)$ decreases with increasing k_{sep}. This tendency is consistent with the assumption that the magnitude of the MFEs on $R(B)$ is determined mainly by the relative magnitude of k_{rlx} and k_{sep} for the geminate BRIP. The variation of viscosity also alters k_{rlx} through the above-mentioned τ_C. In the short correlation time regime,[41b] the shorter τ_C gives the larger k_{rlx} values at high fields, which results in the smaller MFEs on $R(B)$.

It was reported that addition of a paramagnetic species quenched the MFEs on the lifetime or the escaped radical yield due to the RM.[51] In the reaction of ^{3}MPTZ* with **A1**−**R**· in EtOH, addition of $MnCl_2$ (6×10^{-3} M) reduced ϕ_{FI} at any B examined ($0 \le B \le 1.7$ T),[52] although MFEs were still observed (Figure S2). On the other hand, addition of diamagnetic $ZnCl_2$ (8×10^{-3} M) somewhat increased ϕ_{FI}, which was probably due to the salt effect, as in the case of ^{n}Bu$_4$NBF$_4$. Thus, the reduction of ϕ_{FI} in the presence of $MnCl_2$ can be attributed to the acceleration of the spin relaxation of BRIP. The degree of quenching of the MFEs was smaller than that observed for the RPs previously reported,[51] suggesting that the intrapair spin relaxation of the BRIP, irrespective of Mn^{2+}, should be dominant at this concentration of $MnCl_2$.

Decay of An$^{\bullet-}$−*R*·. In the reaction of ^{3}MPTZ* with **A1**−**R**·, we found an additional process which exhibited MFEs. Figure 6A shows the $A_{365}(t)$ curves observed for the same reaction as

Figure 3B. Each of the $A_{365}(t)$ curves was mainly due to the absorption of $\mathbf{A1}^{\bullet-}-\mathbf{R}^{\bullet}$, although the T−T absorption of ^{3}MPTZ* was overlapped with it at the initial stage ($t < 1\ \mu$s). A comparison of Figures 6A and 3B shows that the decay of $\mathbf{A1}^{\bullet-}-\mathbf{R}^{\bullet}$ is much faster than that of $MPTZ^{\bullet+}$. This result indicates that $\mathbf{A1}^{\bullet-}-\mathbf{R}^{\bullet}$ is consumed through not only bimolecular reaction with $MPTZ^{\bullet+}$ but also a unimolecular process. This process is intramolecular ET from the $\mathbf{A1}^{\bullet-}$ part to the TEMPO moiety, which is thermodynamically favorable especially in hydroxylic solvents (Table 1)[53]

$$^3(\mathbf{A1}^{\bullet-}-\mathbf{R}^{\bullet}) \leftrightarrows {}^1(\mathbf{A1}^{\bullet-}-\mathbf{R}^{\bullet}) \quad (8)$$

$$^1(\mathbf{A1}^{\bullet-}-\mathbf{R}^{\bullet}) \rightarrow {}^1(\mathbf{A1}-\mathbf{R}^{-}) \quad (9)$$

As seen in Figure 6A, the decay rate of $\mathbf{A1}^{\bullet-}-\mathbf{R}^{\bullet}$ decreased with increasing B from 0 to 1.7 T. This MFE can be explained as follows: The reaction 9 occurs only from the S state. As B increases, the rate of T−S conversion (process 8) decreases because of the increase in energy gap between the $T_{\pm1}$ states and the S and T_0 states. Furthermore, under high fields, the free ions are predominantly formed from the $Q_{\pm3/2}$ states of BRIP, which means that $\mathbf{A1}^{\bullet-}-\mathbf{R}^{\bullet}$ is initially populated more in the $T_{\pm1}$ states than in the S and T_0 states. Thus, the lifetime of $\mathbf{A1}^{\bullet-}-\mathbf{R}^{\bullet}$ should be lengthened with increasing B.

In the reaction of $\mathbf{A3}-\mathbf{R}^{\bullet}$, the decay of $\mathbf{A3}^{\bullet-}-\mathbf{R}^{\bullet}$ monitored at 720 nm (Figure 6B) was parallel to that of $MPTZ^{\bullet+}$ (Figure 3C). This fact indicates that both of these free ions disappeared through only the bimolecular backward ET reaction. $\mathbf{A2}^{\bullet-}-\mathbf{R}^{\bullet}$ decayed slightly faster than $MPTZ^{\bullet+}$ in a time region of 1−8 μs. The above results indicate that the rate of intramolecular ET (reaction 9) of $\mathbf{An}^{\bullet-}-\mathbf{R}^{\bullet}$ largely decreased in the order of $\mathbf{A1}^{\bullet-}-\mathbf{R}^{\bullet} > \mathbf{A2}^{\bullet-}-\mathbf{R}^{\bullet} > \mathbf{A3}^{\bullet-}-\mathbf{R}^{\bullet}$, as the reducing power of the radical anion moiety ($\mathbf{An}^{\bullet-}$) was diminished (Table 1).

Conclusion

In the present study, we observed a new type of MFE in the photochemical reactions of MPTZ with spin-doublet electron acceptors $\mathbf{An}-\mathbf{R}^{\bullet}$ in homogeneous fluid solutions. In this system, ^{3}MPTZ* was quenched by $\mathbf{An}-\mathbf{R}^{\bullet}$ through two processes: (i) T−D quenching and (ii) ET to give BRIP ($[MPTZ^{\bullet+}\ \mathbf{An}^{\bullet-}-\mathbf{R}^{\bullet}]$) in either the Q or D state. These BRIPs undergo backward ET only from the D state, while the remaining ones separate to give free ions. The ϕ_{FI} values were much lower than those observed in the ET reactions with the corresponding spin-singlet acceptors $\mathbf{An}$ at $B = 0$ T. As B increases, however, the ϕ_{FI} values of the reactions with $\mathbf{An}-\mathbf{R}^{\bullet}$ dramatically increased. The spin dynamics of BRIPs is summarized as follows: (i) When the Q and D states are nearly degenerate ($|J| \leq |A_{HFC}|, |D'|$), they are effectively interconverted through the HFC and electron spin dipolar interactions. (ii) Under high fields ($g\beta B \gg |J|, |A_{HFC}|, |D'|$), the conversion from the $Q_{\pm3/2}$ states to the $Q_{\pm1/2}$ or $D_{\pm1/2}$ states takes place through the spin relaxation. The observed MFEs are explained by the RM, that is, the magnetically induced changes in k_{rlx}. The faster spin relaxation in comparison with RIP ($[MPTZ^{\bullet+}\ \mathbf{An}^{\bullet-}]$) is due to the electron spin dipolar interaction within $\mathbf{An}^{\bullet-}-\mathbf{R}^{\bullet}$. Competition of the Q−D conversion with the separation for BRIP is crucial for determining the magnitude of MFEs.

Acknowledgment. We thank Ms. Masae Nagano for preparation of $MPTZ^{\bullet+}(ClO_4^-)$. Y.M. thanks for financial support "President's Special Research Grant" of RIKEN.

Supporting Information Available: Synthetic procedures and spectral data for $\mathbf{A2}-\mathbf{R}^{\bullet}$, $\mathbf{A3}-\mathbf{R}^{\bullet}$, and **A4**, and two figures representing results for MFEs (PDF). This material is available free of charge via the Internet at http://pubs.acs.org.

References and Notes

(1) Steiner, U. E.; Ulrich, T. *Chem. Rev.* **1989**, *89*, 51−147.

(2) Hayashi, H. *Dynamic Spin Chemistry*; Nagakura, S., Hayashi, H., Azumi, T. Eds.; Kodansha-Wiley: Tokyo, New York, 1998; Chapter 2.

(3) Fujiwara, Y.; Nakagaki, R.; Tanimoto, Y. *Dynamic Spin Chemistry*; Nagakura, S., Hayashi, H., Azumi, T. Eds.; Kodansha-Wiley: Tokyo, New York, 1998; Chapter 3.

(4) (a) Staerk, H.; Razi Naqvi, K. *Chem. Phys. Lett*. **1977**, *50*, 386−388. (b) Sakaguchi, Y.; Hayashi, H. *Chem. Phys. Lett*. **1995**, *245*, 591−597. (c) Wakasa, M.; Hayashi, H. *J. Phys. Chem*. **1996**, *100*, 15640−15643. (d) Wakasa, M.; Nishizawa, K.; Abe, H.; Kido, G.; Hayashi, H. *J. Am. Chem. Soc*. **1999**, *121*, 9191−9197.

(5) (a) Blättler, C.; Jent, F.; Paul, H. *Chem. Phys. Lett*. **1990**, *166*, 375−380. (b) Goudsmit, G.-H.; Paul, H.; Shushin, A. I. *J. Phys. Chem*. **1993**, *97*, 13243−13249. (c) Kawai, A.; Okutsu, T.; Obi, K. *J. Phys. Chem*. **1991**, *95*, 9130−9134. (d) Kawai, A.; Obi, K. *J. Phys. Chem*. **1992**, *96*, 5701−5704. (e) Kobori, Y.; Mitsui, M.; Kawai, A.; Obi, K. *Chem. Phys. Lett*. **1996**, *252*, 355−361. (f) Kobori, Y.; Takeda, K.; Tsuji, K.; Kawai, A.; Obi, K. *J. Phys. Chem. A* **1998**, *102*, 5160−5170. (g) Corvaja, C.; Maggini, M.; Prato, M.; Scorrano, G.; Venzin, M. *J. Am. Chem. Soc*. **1995**, *117*, 8857−8858.

(6) (a) Imamura, T.; Onitsuka, O.; Obi, K. *J. Phys. Chem*. **1986**, *90*, 6741−6744. (b) Fujisawa, J.-I.; Ohba, Y.; Yamauchi, S. *J. Phys. Chem. A* **1997**, *101*, 434−439. (c) Fujisawa, J.-I.; Ishii, K.; Ohba, Y.; Yamauchi, S.; Fuhs, M.; Möbius, K. *J. Phys. Chem. A* **1997**, *101*, 5869−5876. (d) Saiful, I. SM; Fujisawa, J.-I.; Kobayashi, N.; Ohba, Y.; Yamauchi, S. *Bull. Chem. Soc. Jpn*. **1999**, *72*, 661−667.

(7) (a) Corvaja, C.; Maggini, M.; Scorrano, G.; Toffoletti, A. *Appl. Magn. Reson*. **1997**, *12*, 477−493. (b) Ishii, K.; Fujisawa, J.-I.; Adachi, A.; Yamauchi, S.; Kobayashi, N. *J. Am. Chem. Soc*. **1998**, *120*, 3152−3158. (c) Ishii, K.; Hirose, Y.; Kobayashi, N. *J. Phys. Chem. A* **1999**, *103*, 1986−1990. (d) Ishii, K.; Ishizaki, T.; Kobayashi, N. *J. Phys. Chem. A* **1999**, *103*, 6060−6062.

(8) (a) Faulkner, L. R.; Tachikawa, H.; Bard, A. J. *J. Am. Chem. Soc*. **1972**, *94*, 691−699. (b) Tachikawa, H.; Bard, A. J. *Chem. Phys. Lett*. **1974**, *26*, 10−15, 246−251. (c) Razi Naqvi, K.; Staerk, H.; Gillbro, T. *Chem. Phys. Lett*. **1977**, *49*, 160−164. (d) Iwasaki, Y.; Maeda, K.; Murai, H. The Sixth International Symposium on Magnetic Field and Spin Effects in Chemistry and Related Phenomena, Emmetten, Switzerland, 1999, Book of Abstracts p. 67.

(9) Johnson, R. C.; Merrifield, R. E. *Phys. Rev. B* **1970**, *1*, 896−902.

(10) Kearns, D. R.; Stone, A. J. *J. Chem. Phys*. **1971**, *55*, 3383−3389.

(11) Atkins, P. W.; Evans, G. T. *Mol. Phys*. **1975**, *29*, 921−935.

(12) Schulten, K. *J. Chem. Phys*. **1984**, *80*, 3668−3679.

(13) (a) Shushin, A. I. *Z. Phys. Chem*. **1993**, *182*, 9−18. (b) Shushin, A. I. *Chem. Phys. Lett*. **1993**, *208*, 173−178.

(14) (a) Step, E. N.; Buchachenko, A. L.; Turro, N. J. *J. Am. Chem. Soc*. **1994**, *116*, 5462−5466. (b) Buchachenko, A. L.; Ruban, L. V.; Step, E. N.; Turro, N. J. *Chem. Phys. Lett*. **1995**, *233*, 315−318. (c) Buchachenko, A. L.; Berdinsky, V. L. *J. Phys. Chem*. **1996**, *100*, 18292−18299. (d) Buchachenko, A. L.; Berdinsky, V. L. *Chem. Phys. Lett*. **1998**, *298*, 279−284.

(15) Conti, F.; Corvaja, C.; Maggini, M.; Piu, F.; Scorrano, G.; Toffoletti, A. *Appl. Magn. Reson*. **1997**, *13*, 337−346.

(16) Mori, Y.; Sakaguchi, Y.; Hayashi, H. *Chem. Phys. Lett*. **1998**, *286*, 446−451.

(17) Mori, Y.; Sakaguchi, Y.; Hayashi, H. *Chem. Phys. Lett*. **1999**, *301*, 365−371.

(18) Ali, S. S.; Maeda, K.; Murai, H.; Azumi, T. *Chem. Phys. Lett*. **1997**, *267*, 520−524.

(19) Belf, L. J. U.S. Patent 3,401,191; 1968.

(20) Fujita, H.; Yamauchi, J. *J. Heterocycl. Chem*. **1980**, *17*, 1053−1056.

(21) (a) Complexation of Na^+ with the cryptand prevents ion pairing. (b) Hosoi, H.; Mori, Y.; Masuda, Y. *Chem. Lett*. **1998**, 177−178.

(22) *PCPro-K*, Global Analysis and Simulation Package for Windows95, Applied Photophysics Ltd., 1996.

(23) Astashkin, A. V.; Sakaguchi, Y. *J. Chem. Phys*. **1997**, *106*, 9190−9200.

(24) Moroi. Y.; Braun, A. M.; Grätzel, M. *J. Am. Chem. Soc*. **1979**, *101*, 567−572.

(25) Biehl, E. R.; Chiou, H.-S.; Keepers, J.; Kennard, S.; Reeves, P. C. *J. Heterocycl. Chem*. **1975**, *12*, 397−399.

(26) Sakaguchi, Y.; Hayashi, H. *J. Phys. Chem. A*, **1997**, *101*, 549−555.

(27) Kuzmin, V. A.; Takikov, A. S. *Chem. Phys. Lett.* **1978**, *53*, 606−610.

(28) The D_1 energy of TEMPO was estimated as 18 000 cm^{-1} (2.2 eV)[5c] in benzene, based on the absorption spectrum. In 2-PrOH, the absorption maximum was blue shifted by 800 cm^{-1} compared with that in benzene.

(29) (a) For the reaction of **A1**−**R**•, the polarization of the sharp signal changed from emission to absorption at ca. 800 ns and then decayed to the baseline in 2.5 μs. These results suggested that not only the T−D quenching but also the spin-selective backward ET of BRIP should generate polarization of the TEMPO moiety of **A1**−**R**•. (b) For the reaction of **A3**−**R**•, a broad signal was also observed in a higher field than the center of the three-line signal, but it exhibited emissive polarization. The mechanism of the polarization observed in the reactions of ^{3}MPTZ* with **A***n*−**R**• is under investigation. (c) A theoretical work on TREPR spectra of similar three-spin systems was reported. Salikhov, K. M.; van der Est, A. J.; Stehlik, D. *Appl. Magn. Reson.* **1999**, *16*, 101−134.

(30) (a) Under the conditions of our TREPR measurements, the decay of signal to the baseline before the laser pulse corresponds to the establishment of the thermal equilibrium. (b) The spin−lattice relaxation time of TEMPO was reported to be 340 ns in 2-PrOH at 270 K.[5f]

(31) (a) $\Delta G_{ET} = -E_T + E_{ox} - E_{red} - e^2/4\pi\epsilon_0\epsilon_r R + e^2/2(1/r_+ + 1/r_-)(1/4\pi\epsilon_0\epsilon_r^{PrOH} - 1/4\pi\epsilon_0\epsilon_r^{MeCN})$. The following values were assumed: R = 7.0 Å, r_+ = 3.5 Å, r_- = 3.0 Å. (b) Rehm, D.; Weller, A. *Isr. J. Chem.* **1970**, *8*, 259−271.

(32) For ^{3}MPTZ*, $\epsilon_{465} = 2.3 \times 10^4$ M^{-1} cm^{-1} in aqueous micellar solution;[24] for MPTZ$^{\bullet+}$, $\epsilon_{516} = 9.18 \times 10^4$ M^{-1} cm^{-1} in aqueous micellar solution,[24] $\epsilon_{513} = 9.7 \times 10^4$ M^{-1} cm^{-1} in $MeNO_2$−CF_3CO_2H,[25] and $\epsilon_{520} = 9.7 \times 10^4$ M^{-1} cm^{-1} in CH_2Cl_2 (this work).

(33) (a) The lower ϕ_{FI} value of **A3** than those of the other acceptors may be due to quenching through triplet energy transfer, although the T−T absorption of **A3** (λ_{max} 560 and 510 nm) was not detected. The triplet excitation energy of **A3** is probably close to that of MPTZ (E_T = 2.64 eV), because the phosphorescence spectrum of *N*,*N*′-dipentyl-pyromellitic diimide was reported to show a broad band around 500 nm. (b) Martens, F. M.; Verhoeven, J. W.; Varma, C. A. G. O.; Bergwerf, P. *J. Photochem.* **1983**, *22*, 99−113.

(34) Sano, H.; Tachiya, M. *J. Chem. Phys.* **1979**, *71*, 1276−1282.

(35) (a) Niwa, T.; Kikuchi, K.; Matsushita, N.; Hayashi, M.; Katagiri, T.; Takahashi, Y.; Miyashi, T. *J. Phys. Chem.* **1993**, *97*, 11960−11964. (b) Inada, T. N.; Miyazawa, C. S.; Kikuchi, K.; Yamauchi, M.; Nagata, T.; Takahashi, Y.; Ikeda, H.; Miyashi, T. *J. Am. Chem. Soc.* **1999**, *121*, 7211−7219.

(36) (a) The observed k_{sep} value for a solvent-separated IP consisting of oppositely charged univalent ions with ionic radii of 3−4 Å has been reported to be (0.5−2) $\times 10^9$ s^{-1} in MeCN at room temperature.[36b−g] Equation 6 gives a calculated k_{sep} value of 1.8×10^9 s^{-1} for such IP in MeCN at 293 K, which agrees with the observed value. (b) Weller, A. *Z. Phys. Chem. (Munich)* **1982**, *130*, 129−138. (c) Mataga, N.; Shioyama, H.; Kanda, Y. *J. Phys. Chem.* **1987**, *91*, 314−317. (d) Mataga, N.; Asahi, T.; Kanda, Y.; Okada, T. *Chem. Phys.* **1988**, *127*, 249−261. (e) Peters, K. S.; Lee, J. *J. Phys. Chem.* **1992**, *96*, 8941−8945. (f) Peters, K. S.; Lee, J. *J. Am. Chem. Soc.* **1993**, *115*, 3643−3646. (g) Peters, K. S.; Li, B. *J. Phys. Chem.* **1994**, *98*, 401−403.

(37) The recombination of free ions involves the T−S conversion of RIP. The observed bimolecular decay rates of free MPTZ$^{\bullet+}$ exhibited MFEs quite similar to those on the $R(B)$ values. See ref 26.

(38) Because of the somewhat larger molecular size, the separation to free ions of BRIP involving **A***n*$^{\bullet-}$−**R**• (n = 1 or 2) is slower than that of RIP involving **A***n* (n = 1 or 2). We examined ϕ_{FI} and its B-dependence for ET from ^{3}MPTZ* to **A4** whose molecular size is similar to that of **A1**−**R**•. At B = 0 T, ϕ_{FI} for the reaction of **A4** is about 0.95 of that for the reaction of **A1**. The MFEs on $R(B)$ for the reaction of **A4** were the same as those for the reaction of **A1** at B = 0−1.7 T. Furthermore, the molecular sizes of **A3**−**R**• and **A3** are not so different, but significant differences were observed in ϕ_{FI} and MFEs. Thus, the difference in molecular size among the acceptors is not a major factor controlling the ϕ_{FI} value and the magnitude of MFEs.

(39) In the reaction of ^{3}MPTZ* with **A1**−**R**•, free **A1**$^{\bullet-}$−**R**• was consumed not only through the bimolecular recombination with MPTZ$^{\bullet+}$ but also through a unimolecular decomposition. To exclude the contribution of the absorbance due to **A1**$^{\bullet-}$−**R**•, the $R(B)$ value was defined as $R(B) = A_{520}(1.8\ \mu s, B)/A_{520}(1.8\ \mu s, 0\ T)$, since **A1**$^{\bullet-}$−**R**• had almost disappeared by 1.8 μs.

(40) The k_q values at $B > 0$ T were obtained as $k_q = (k_{obs} - k_0)/(1 \times 10^{-3}$ M). Here, k_{obs} was the observed decay rate of ^{3}MPTZ* in the presence of TEMPO (1×10^{-3} M) at B and k_0 ($= 1.5 \times 10^5$ s^{-1}) was the decay rate in the absence of TEMPO, where k_0 was independent of B.

(41) (a) Atkins, P. W.; Evans, G. T. *Mol. Phys.* **1974**, *27*, 1633−1644. (b) Abragam, A. *The Principles of Nuclear Magnetism*; Oxford University Press: London, 1961; Chapter VIII.

(42) (a) Igarashi, M.; Sakaguchi, Y.; Hayashi, H. *Mol. Phys.* **1994**, *82*, 1165−1179. (b) Nakamura, Y.; Igarashi, M.; Sakaguchi, Y.; Hayashi, H. *Chem. Phys. Lett.* **1994**, *217*, 387−392. (c) Igarashi, M.; Meng, Q.-X.; Sakaguchi, Y.; Hayashi, H. *Mol. Phys.* **1995**, *84*, 943−955. (d) Nishizawa, K.; Sakaguchi, Y.; Hayashi, H.; Abe, H.; Kido, G. *Chem. Phys. Lett.* **1997**, *267*, 501−506. (e) Fujiwara, Y.; Yoda, K.; Tomonari, T.; Aoki, T.; Akimoto, Y.; Tanimoto, Y. *Bull. Chem. Soc. Jpn.* **1999**, *72*, 1705−1715. (f) Misra, A.; Haldar, M.; Chowdhury, M. *Chem. Phys. Lett.* **1999**, *305*, 63−70.

(43) (a) Fujiwara, Y.; Aoki, T.; Yoda, K.; Cao, H.; Mukai, M.; Haino, T.; Fukazawa, Y.; Tanimoto, Y.; Yonemura, H.; Matsuo, T.; Okazaki, M. *Chem. Phys. Lett.* **1996**, *259*, 361−367. (b) Tanimoto, Y.; Tanaka, H.; Fujiwara, Y.; Fujiwara, M. *J. Phys. Chem. A*, **1998**, *102*, 5611−5615.

(44) Hayashi, H.; Nagakura, S. *Bull. Chem. Soc. Jpn.* **1984**, *57*, 322−328.

(45) Spin relaxation induced by the intermolecular interactions between BRIP and **A***n*−**R**• can be ruled out from the fact that the $R(B)$ values for the reaction of ^{3}MPTZ* with **A1** in the presence of 1 mM of TEMPO were almost the same as the corresponding values without TEMPO.

(46) The backward ET of ^{2}BRIP (process f in Scheme 2) is not necessarily spin allowed. Buchachenko and Berdinsky theoretically studied the following reaction I, where [R_1• R_2• R_3•] is an intermediate having three radical centers, and ^{1}(R_1−R_2) is a product.[14c,d]

^{2}[R_1• R_2• R_3•] → ^{1}(R_1−R_2) + R_3• (I)

^{2}[^{1}(R_1• •R_2) R_3•] ($D^S_{\pm1/2}$ state) → ^{1}(R_1−R_2) + R_3• (II)

^{2}[^{3}(R_1• •R_2) R_3•] ($D^T_{\pm1/2}$ state) ⇆ ^{2}[^{1}(R_1• •R_2) R_3•] ($D^S_{\pm1/2}$ state) (III)

In the $D^S_{\pm1/2}$ state, the (R_1• •R_2) pair is singlet and can react to give the product (process II), while in the $D^T_{\pm1/2}$ state, the pair is triplet and cannot react. According to their theory, oscillations between the $D^T_{\pm1/2}$ and $D^S_{\pm1/2}$ states (process III) are induced by the difference in J value, $\Delta J = |J_{13} - J_{23}|$, where J_{ij} (i, j = 1, 2, 3) is the exchange interaction between radical centers i and j. This scheme is applicable to the backward ET of ^{2}BRIP, where R_1 = MPTZ$^{\bullet+}$, R_2 = **A***n*$^{\bullet-}$, and R_3 = **R**•. In a mutual orientation, where MPTZ$^{\bullet+}$ is located closer to **A***n*$^{\bullet-}$ than to **R**•, it is likely that $|J_{13}| \ll |J_{23}|$. In such a case, the nonzero ΔJ induces the $D^T_{\pm1/2}$−$D^S_{\pm1/2}$ mixing effectively. Thus, once ^{4}BRIP is converted to ^{2}BRIP, the latter rapidly acquires $D^S_{\pm1/2}$ character through this $D^T_{\pm1/2}$−$D^S_{\pm1/2}$ mixing and undergoes the backward ET reaction.

(47) (a) Weir, D. J.; Depew, M. C.; Wan, J. K. S. *Res. Chem. Intermed.* **1990**, *14*, 269−282. (b) $|D|$ value for ^{3}MPTZ* is unknown. However, the TREPR spectrum observed in the quenching of the T_1 state of unsubstituted phenothiazine by TEMPO in 2-PrOH also exhibits a net emissive three-line signal with an almost 1:1:1 ratio due to TEMPO.[48c] (c) He, G.; Chen, C.; Yang, J.; Xu, G. *J. Phys. Chem. A* **1998**, *102*, 2865−2869.

(48) (a) The d_{CC} values were determined for the parent neutral radicals **A***n*−**R**•, whose structures were optimized by ROHF calculation with the PM3[48b] method using MOPAC 97.[48c] (b) Stewart, J. J. J. *J. Comput. Chem.* **1989**, *10*, 209−220. (c) WinMOPAC Ver. 2.0, Fujitsu Ltd., Japan, 1997. (d) $|D'|$ and $|E'|$ of **A1**$^{\bullet-}$−**R**• were also estimated using the point−charge approximation with the spin densities obtained for **A1**$^{\bullet-}$ by UHF calculation. The same geometry was used as the case of the point−dipole approximation. The calculated values are $|D'| = 5.65$ and $|E'| = 0.06$ mT for the extended conformer, while $|D'| = 8.09$ and $|E'| = 0.21$ mT for the folded one.

(49) The k_{sep} value for a pair without Coulombic force between its components is estimated as $k_{sep} = D_t/r_q^2$.[34,35b] Assuming that the T−D quenching occurs at contact distance ($r_q \sim 7$ Å), k_{sep} is calculated to be 1.1×10^9 s^{-1} in 2-PrOH at 293 K, which is much larger than the corresponding value (8×10^7 s^{-1}) for [MPTZ$^{\bullet+}$ **A***n*$^{\bullet-}$−**R**•] estimated with eq 6a.

(50) (a) Yabe, T.; Kochi, J. K. *J. Am. Chem. Soc.* **1992**, *114*, 4491−4500. (b) Hubig, S. M.; Rathore, R.; Kochi, J. K. *J. Am. Chem. Soc.* **1999**, *121*, 617−626.

(51) (a) Sakaguchi, Y.; Hayashi, H. *Chem. Phys. Lett.* **1984**, *106*, 420−424. (b) Sakaguchi, Y.; Hayashi, H. *Chem. Phys.* **1992**, *162*, 119−129. (c) Wakasa, M.; Sakaguchi, Y.; Hayashi, H. *Mol. Phys.* **1994,** *83*, 613−618. (d) Wakasa, M.; Hayashi, H.; Mikami, Y.; Takeda, T. *J. Phys. Chem.* **1995**, *99*, 13181−13186. (e) Turro, N. J.; Lei, X.; Gould, I. R.; Zimmt, M. B. *Chem. Phys. Lett.* **1985**, *120*, 397−400. (f) Levin, P. P.; Kuzmin, V. A. *Chem. Phys.* **1992**, *162*, 79−93.

(52) The decay rate of ^{3}MPTZ* in the presence of $MnCl_2$ was slightly larger than that in its absence, but most of ^{3}MPTZ* (> 90%) was quenched by **A1**−**R**•. Although Mn^{2+} may accelerate the T−D quenching, the effect on the T−D quenching efficiency is probably much smaller than that on ϕ_{sep}, because the lifetime of [^{3}MPTZ* **A1**−**R**•] is shorter than that of [MPTZ$^{\bullet+}$ **A1**$^{\bullet-}$−**R**•].[49]

(53) (a) The reduction product (R^-) of TEMPO (R•) is readily protonated to give the corresponding hydroxylamine (RH), which exhibits no optical absorption in visible region. Fish, J. R.; Swarts, S. G.; Sevilla, M. D.; Malinski, T. *J. Phys. Chem.* **1988**, *92*, 3745−3751. (b) TEMPO is reduced more easily in hydroxylic solvents than in aprotic solvents. For example, the reduction potential of TEMPO measured in MeOH is less negative by 1.2 V than that obtained in THF. Green, S.; Fox, M. A. *J. Phys. Chem.* **1999**, *103*, 5416−5424.

(54) *Handbook of Chemistry and Physics*, 77th edition; Lide, D. R. Ed.; CRC Press: Boca Raton, FL, 1996; pp 6−151.